Chalcogenide Letters Vol. 18, No. 11, November 2021, p. 735 - 743

# Hydrothermal synthesis and tribological properties of $WS_2$ microspheres

X. H. Zhang[a], Z. Wang[b,*], H. Tan[a], M. Q. Xue[c]
[a]*School of Mechanical Engineering, Jiangsu University of Technology, Changzhou 213001, Jiangsu Province, China*
[b]*Jiangsu Laboratory of Lake Environment Remote Sensing Technologies，Huaiyin Institute of Technology, HuaiAn, 223003, Jiangsu Province, China.*
[c]*Changzhou Institute of Industry Technology, Changzhou, 213164, Jiangsu Province, China*

In this work, $WS_2$ microspheres were synthesized through a facile hydrothermal route. The as-synthesized samples were characterized by powder X-ray powder diffraction (XRD), X-ray photoelectron spectroscopy (XPS), energy-dispersive spectroscopy and scanning electron microscopy (SEM). The XRD spectrum of the sample is indexed to hexagonal $WS_2$. SEM graphics of the products reveal that the $WS_2$ microspheres with diameters of about 2-8 μm were synthesized. The tribological properties of $WS_2$ microspheres as oil additives were tested on a ball-disk tribometer. Under the given experimental conditions, the friction coefficient of the oil containing $WS_2$ is lower than that of the base oil. The formation of rolling friction between the friction pairs and the smooth friction film on the wear surface are considered to be the reason for the good lubricating effect of $WS_2$ microspheres as an additive.

(Received September 12, 2021; Accepted November 18, 2021)

*Keywords:* $WS_2$, Microspheres, Tribological performance

## 1. Introduction

According to recent research by Holmberg et al., the friction of the engine, gearbox, tires, auxiliary equipment and brakes of heavy vehicles consumes 33% of fuel energy [1], friction in automobiles consumes 28% of fuel energy [2], and the energy consumed by friction in the entire paper mill accounts for 15-25% [3]. Therefore, many attempts have been made to introduce various methods to overcome friction. Lubrication is known to be one of the most effective ways to reduce friction and wear [4]. Lubrication oil additives have an important influence on the performance of lubrication. These additives are active ingredients and can be added to the base oil during the mixing process to enhance the existing properties of the base oil or impart new characteristics that the base oil lacks [5-6]. In modern industry, the ever-increasing demand for mechanical life and efficiency has stimulated research on better performance lubricant additives.

In the past few decades, the transition metal dichalcogenides $MX_2$ (M=Mo, W, Ti, V, Nb, and Ta, X=S, Se) have attracted great attention due to its unique structure and superior performance. It is well known that transition metal dichalcogenides have a sandwich structure formed by stacking X-M-X layers. The layers are loosely combined only by van der Waals forces and are easy to split,

* Corresponding authors: wangze@jsut.edu.cn
https://doi.org/10.15251/CL.2021.1811.735

but there is a strong bonding force within the layers. This unique structure makes $MX_2$ exhibit good mechanical [7], physical [8], optical [9] and electrical [10] properties and have numerous applications such as solid lubricants, catalysis, electrocatalysis, high-density batteries and efficient solar energy cells [11–20].

As a member of the $MX_2$ family, $WS_2$ has been used in professional applications for decades as a solid lubricant or additive for lubricating oils and greases. And the tribological properties of $WS_2$ micro-nano materials with different morphologies have been extensively studied. For example, R. Tenne [21-23] and Yang [24] et al. researched lubricating performance of inorganic fullerene-like $WS_2$ nanoparticles. Zhang [25] reported the tribological properties of $WS_2$ nanorods as lubricating oil additive. Wu [26] et al. studied the tribological properties of tungsten disulfide hollow spheres in liquid paraffin. Wu [27] et al. tested the tribological properties of lubricating oil containing micro/nanoscale $WS_2$. Zhang [4, 28] et al. compared and analyzed the tribological properties of $WS_2$ hexagonal nanosheets and nanoflowers. The above studies proved that the tribological properties of $WS_2$ are related to the morphology and size of the material. Therefore, many attentions have been focused on the synthesis of $WS_2$ nanomaterials with desired size and morphology through thermal decomposition, solid–gas reaction method, chemical vapor condensation, hydrothermal synthesis and soon [29–33]. Among these methods, the hydrothermal method has proven to be a convenient, effective and promising method to adjust the size and morphology of $WS_2$ [34].

In this study, the $WS_2$ microspheres were prepared by a facile hydrothermal reaction method and the tribological properties of $WS_2$ microspheres as additives in the base oil were also investigated.

## 2. Experimental

### 2.1. Synthesis of WS2 microspheres

The raw materials, thioacetamide ($C_2H_5NS$), ammonium tungstate ($(NH_4)6H_2W_{12}O_{40}\cdot xH_2O$) and oxalic acid ($H_2C_2O_4\cdot 2H_2O$), were purchased from Aladdin Chemical Reagent Company. All reagents were of analytical grade and were used without further purification. In the typical synthesis, 0.76g of ammonium tungstate and 0.75g of thioacetamide were first dissolved in 30mL of deionized water by magnetic stirring for 15 min. Then add 0.284g of oxalic acid to the above solution and continue stirring for 15 minutes. Then the solution was transferred into a 50 ml stainless steel autoclave, sealed and maintained at 240℃ for 24 h. After naturally cooling to room temperature, the final black product was collected by centrifuged and washed three times with deionized water and ethanol each, and dried in an oven at 60 ° C for 12 hours.

### 2.2. Materials characterization

The X-ray diffraction (XRD) patterns were recorded using Bruker-AXS D8 X-ray diffractometer with Cu Kα radiation (λ=0.1546 nm). The X-ray photoelectron spectroscopy (XPS) was determined by a Thermo ESCALAB 250X electron spectrometer. The morphologies of the as-synthesized samples were observed by the scanning electron microscopy (SEM, JEOL, JSM-6390) equipped with the Energy Dispersive X-ray Spectroscopy detector.

### 2.3. Tribological properties measurement

The prepared $WS_2$ sample was ultrasonically dispersed in the base oil without any active reagents. The UMT-2 ball-disk tribometer was used to study the tribological properties of the base oil with the $WS_2$ sample. The anti-wear and anti-friction performance test were carried out for 600 seconds at 200 rpm and 10-60 N applied load. The 10 mm diameter ball used in the test is made of 440C stainless steel with a hardness of 62 HRC. The disc is made of 45 steel and the size is Ø 30 × 5 mm. The friction coefficient is automatically recorded by a computer, and the wear scar width (WSW) is measured by a metallurgical microscope. The morphology of the worn surface was analyzed by scanning electron microscope (SEM, JSM-5600LV).

## 3. Results and Discussion

### 3.1. Structural and Morphological Characterization of $WS_2$ microspheres

The crystal structure and phase composition of the synthesized sample were confirmed by powder X-ray diffraction. The typical XRD pattern of the prepared $WS_2$ microspheres is shown in Fig. 1a. The peaks at $2\theta = 14.12°$, 32.62°,35.74°, and 43.42° are respectively related to the (002), (100), (102), and (006) planes of $WS_2$, and all the diffraction peaks can be indexed to hexagonal phase of $WS_2$ (JCPDS Card No. 08-0237). EDS spectrum is presented in Fig. 1b, which reveals that the sample consisted of element W and S, no other element is observed. Moreover, the quantification of the peaks shows that the molar ratio of W to S is about 1:1.99, which is almost consistent with the stoichiometric $WS_2$. To further characterize surface element composition and bonding state of the as prepared sample, X-ray photoelectron spectroscopy (XPS) was conducted. The chemical states of W and S in $WS_2$ were confirmed through the high-resolution XPS spectra, as shown in Fig.1c. It can be found that the binding energy of W $4f_{7/2}$ and W $4f_{5/2}$ were 32.80 eV and 34.70 eV, respectively. In addition, a peak of W $5p_{5/2}$ was observed, which was weak but with a higher binding energy (38.40 eV). The binding energies of S $2p_{3/2}$ and S $2p_{1/2}$ were 162.20 eV and 163.50 eV, respectively, both of which were in agreement with the standard values, thereby demonstrating that W and S could exist in states of $W^{4+}$ and $S^{2-}$ [35,36], respectively.

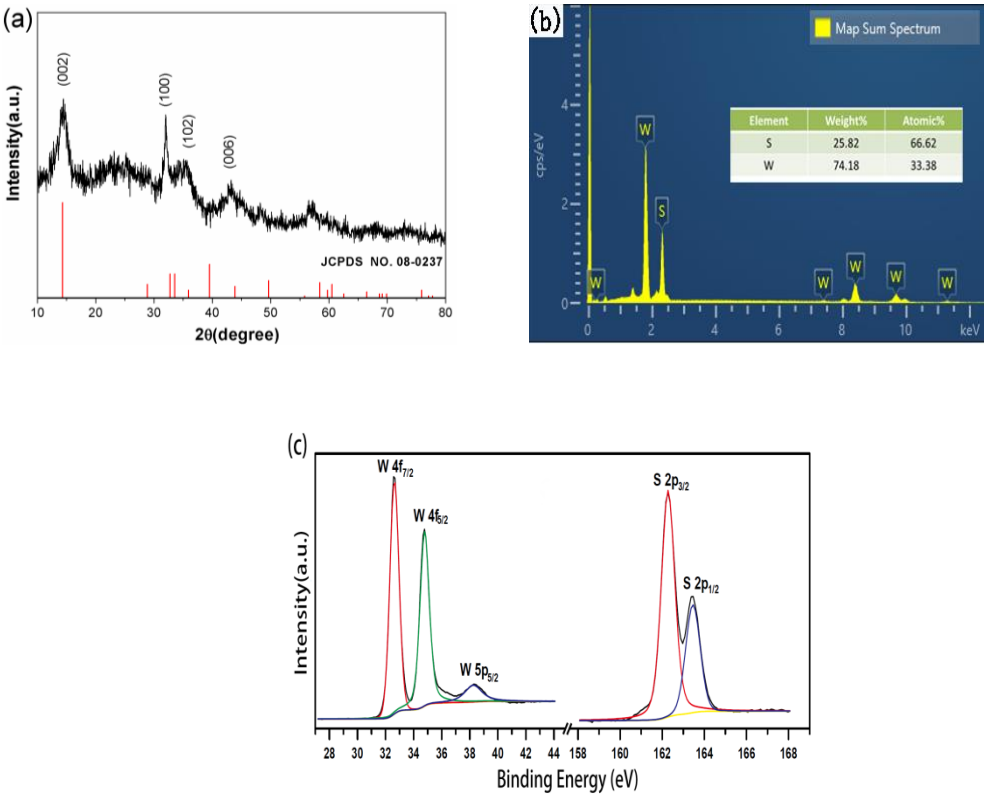


*Fig. 1. (a) XRD pattern, (b) EDS and (c) high resolution XPS spectrum of the as-prepared $WS_2$ microspheres.*

Fig. 2 shows the SEM images and elemental maps of the $WS_2$ samples. In Figure 2a, the low-magnification SEM image shows that the sample is composed of many uniform-sized microspheres, and some of the microspheres are agglomerated. The size of the microspheres is distributed in 2-8 μm. Figure 2b shows a complete microsphere, from which it can be seen that the microsphere is composed of many small $WS_2$ nanosheets. The magnified SEM image (Fig. 2c) clearly shows the morphology of the nanosheets, from which it can be seen that some of the nanosheets are curled into nanorods. Energy dispersive X-ray spectroscopy (EDS) mapping analysis was also performed, as shown in Figure 2d, which proved that S and W are uniformly distributed throughout the microsphere.

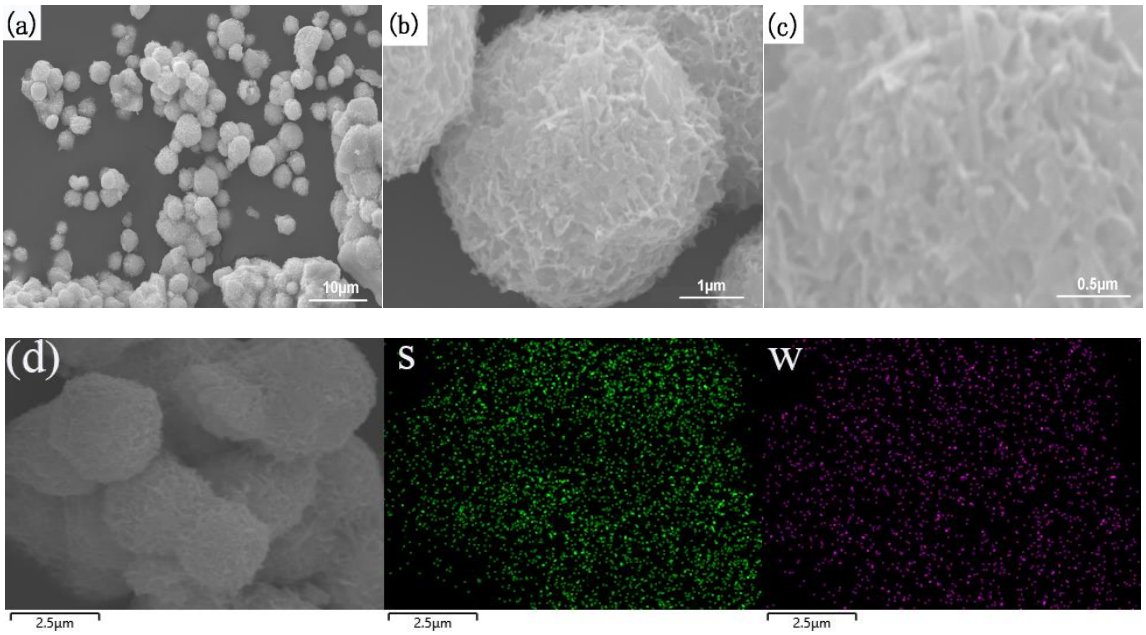


*Fig. 2. FESEM (a,b,c) and elemental maps (d) images of the $WS_2$ microspheres.*

### 3.2. Tribological Performance

The influence of $WS_2$ microspheres concentration on the average friction coefficient was detected by a UMT-2 tribometer. The test was carried out under a load of 10-60 N and a rotating speed of 200 rpm with duration of 10 minutes. Fig. 3a shows the change in the average friction coefficient of the lubricant under different loads. It can be seen that under the test load (10, 20, 40 and 60N), all of the friction coefficients of the base oil with different concentrations of $WS_2$ samples are less than that of pure oil. It has also been observed that the friction coefficient of pure oil increases rapidly under a load above 20 N. While the average friction coefficients for base oil with $WS_2$ microspheres were low and presented a little increase when the applied load is over 40N. In addition, when the concentration of $WS_2$ microspheres is 1.0-1.5 wt%, the friction coefficient is lower and more stable.

Figure 3b shows the width of the wear scar after the disc is lubricated by different lubricating oil samples after 10 minutes of testing under the conditions of a load of 20 N and a speed of 200 rpm. It can be seen that the width of the wear scar of pure oil is 0.485 mm, while the width of the wear scar of the base oil containing 1 wt% $WS_2$ microspheres is 0.32 mm. However, the wear scar widths of the oil with 1.5 and 4 wt% $WS_2$ microspheres are slightly increased. The results can be explained by the fact that too much higher concentration of the nanoparticles exhibited extensive agglomeration, could not enter the contact area easily [37], also could destroy the stability of the colloid system of the base oil [38]. Therefore, the optimum concentration of the synthesized $WS_2$ as an additive in base oil is suggested to be 1 wt%.

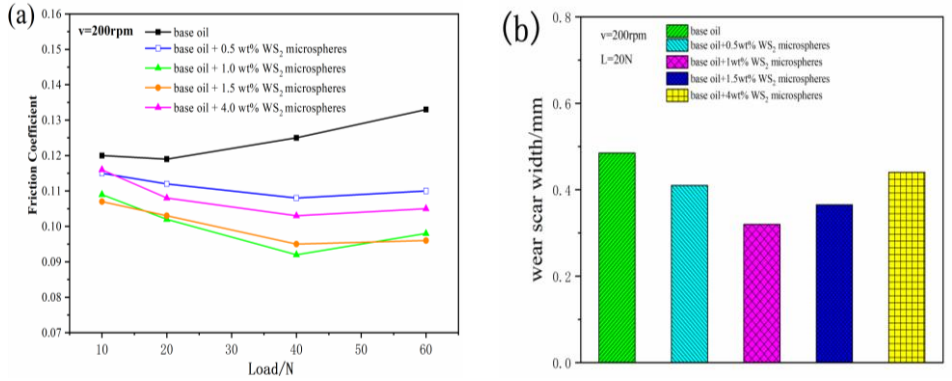


*Fig. 3. (a)Variation of mean friction coefficient, as a function of load and (b) wear scar width on disc specimens lubricated by different oil samples.*

Fig. 4 shows the real-time friction coefficients of the tribo-pairs lubricated by five different oil samples under load of 20 N and rotating speed of 200rpm for 10 min. It is observed that the real-time friction coefficient of the base oil increases with the extension of the test time. While the coefficient of base oil with $WS_2$ microspheres is decreased and the friction coefficient draft is more stable. In addition, after an obvious running-in phase, the friction coefficient of the base oil containing 1-1.5 wt % $WS_2$ microspheres is more stable.

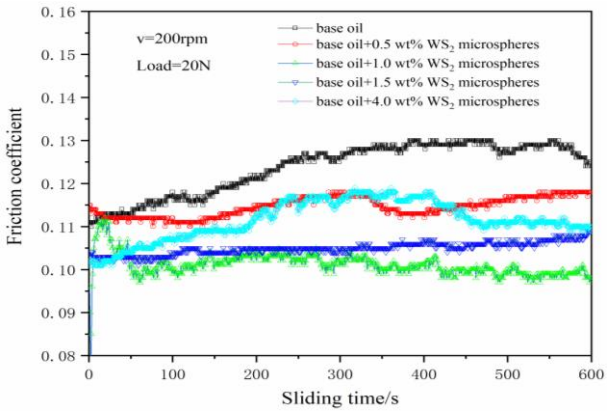


*Fig. 4. Friction coefficient as a function of sliding time lubricated by different oil samples.*

Figure 5 shows the SEM images of the worn surface of steel disc which lubricated by base oil and the base oil with 1.0 wt.% $WS_2$ microspheres at 20 N for 10 min. It can be seen from Figure 5a that the wear surface lubricated with base oil has obvious rough grooves. However, in Figure 5b, the wear surface lubricated with the base oil containing 1.0 wt% $WS_2$ is smoother and shows shallow grooves, which also shows that a protective friction film is produced on the wear surface.

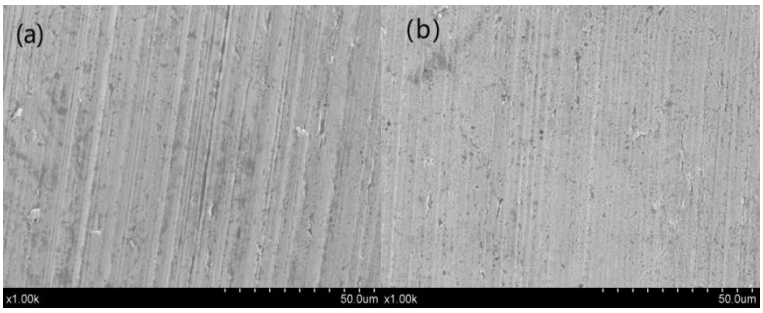


*Fig. 5. SEM images of worn surface lubricated with pure base oil (Fig. 5a) and base oil containing 1 wt% $WS_2$ (Fig. 5b).*

The above results indicate that $WS_2$ microspheres as a lubrication additive can improve the tribological properties of the base oil. The anti-friction and anti-wear mechanisms of nanomaterials as lubricant additives have been discussed in many literatures. For example, Tenne et al. analyzed the antifriction mechanism of inorganic fullerene-like (IF) $WS_2$ hollow particles, and attributed them to the following three factors: (a) rolling friction; (b) the IF nanoparticles serve as spacers, preventing the contact between the asperities of the two mating metal surfaces; (c) third body material transfer [39]. The anti-friction mechanism of $WS_2$ microspheres is similar to this. When $WS_2$ is used as a lubrication additive, $WS_2$ microspheres penetrate into the friction surface with the lubrication oil and are distributed on the surface of the friction pair. The spherical particles first act as a rolling bearing, turning the sliding friction between the friction pairs into rolling friction. After a period of time, the $WS_2$ microspheres are dispersed into many $WS_2$ nanosheets. These nanosheets are adsorbed on the surface of the friction pair and converted into a lubricating film, which further improves the friction condition between the friction pairs.

## 4. Conclusion

In summary, $WS_2$ microspheres with a diameter of about 2-8 μm were successfully prepared by hydrothermal reaction. The experimental results show that the prepared $WS_2$ microspheres can significantly improve the tribological performance of the base oil, and when the concentration of $WS_2$ microspheres is 1-1.5 wt%, the lubricating oil exhibits the best tribological performance.

**Acknowledgements**

This research was supported by the Scientific Research Foundation of Jiangsu University of Technology (KYY18030), Jiangsu Overseas Visiting Scholar Program for University Prominent Young & Middle-aged Teachers and Presidents, the Jiangsu Laboratory of Lake Environment Remote Sensing Technologies (JSLERS-2019-002), the Key Program for Research Team of Changzhou Institute of Industry Technology (ZD201813101003), and Industry University Research Cooperation Project of Jiangsu province.

## References


[1] K. Holmberg, P. Andersson, N. O. Nylund, K. Makela, A. Erdemir, Tribology International **78**, 94 (2014).

[2] K. Holmberg, P. Andersson, A. Erdemir, Tribology International **47**, 221 (2012).

[3] K. Holmberg, R. Siilasto, T. Laitinen, P. Andersson, A. Sberg, Tribology International **62**, 58 (2013).

[4] X. H. Zhang, J. T. Wang, H. X. Xu, H. Tan, X. Ye, Nanomaterials **9**, 840 (2019).

[5] D. Jiao, S. H. Zheng, Y. Z. Wang, R. F. Guan, B. Q. Cao, Applied Surface Science **257**, 5720 (2011).

[6] Z. Chen, X. W. Liu, Y. H. Liu, S. Gunsel, J. B. Luo, Scientific Reports **5**, 12869 (2015).

[7] R. Greenberga, G. Halperina, I. Etsiona, R. Tenne, Tribology Letters **17**(2), 179 (2004).

[8] M. Y. Lu, M. P. Lu, Y. A. Chung, M. J. Chen, Z. L. Wang, L. J. Chen, Journal of Physical Chemistry C **113**, 12878 (2009).

[9] S. X. Cao, C. Zhao, L. L. Peng, Materials Letters **164**, 452 (2016).

[10] J. Bai, B. C. Zhao, J. F. Zhou, J. G. Si, Z. T. Fang, K. Z. Li, H. Y. Ma, J. M. Dai, X. B. Zhu, Y. P. Sun, Small **15**, 1805420 (2019).

[11] G. G. Tang, J. R. Sun, W. Chen, H. Tang, Y. J. Wang, C. S. Li, Micro & Nano Letters **8**(3), 164 (2013).

[12] X. H. Zhang, H. Tang, C. S. Li, S. Chen, Chalcogenide Letters **10**(10), 403(2013).

[13] X. H. Zhang, D.Zhang, H.T. Zhang, H. Tang, C. S. Li, S. Chen, Y. Jin, Chalcogenide Letters **11**(1), 1(2014).

[14] Y. P. Liu, Y. H. Li, F. Peng, Y. Lin, S. Y. Yang, S. S. Zhang, H. J. Wang, Y. H. Cao, H. Yu, Applied Catalysis B: Environmental **241**, 236 (2019).

[15] C. W. Fei, L. X. Cui, H. W. Du, L. N. Gu, G. S. Xu, Y. P. Yuan, New Journal of Chemistry **43**, 9583 (2019).

[16] D. Z. Wang, Z. Pan, Z. Z. Wu, Z. P. Wang, Z. H. Liu, Journal of Power Sources **264**, 229 (2014).

[17] L. Fei, Y. Xu, X. F. Wu, G. Chen, Y. L. Li, B. S. Li, S. G. Deng, S. Smirnov, H. Y. Fan, H. M. Luo, Nanoscale **6**, 3664 (2014).

[18] Y. Wang, D. Z. Kong, S. Z. Huang, Y. M. Shi, M. Ding, Y. V. Lim, T. T. Xu, F. M. Chen, X. J. Li, H. Y. Yang, Journal of Materials Chemistry A **6**, 10813(2018).

[19] Q. Liu, A. Gao, Y. L. Huang, F. Y. Yi, H. H. Chen, S. X. Zhao, H. Y. Chen, R. H. Zeng, Z. Q. Sun, D. Shu, X. N, Song, Journal of Alloys and Compounds **777**, 1176,(2019).

[20] Y. Yuan, H. P. Lv, Q. J. Xu, H. M. Liu, Y. G. Wang, Nanoscale **11**, 4318 (2019).

[21] L. Rapoport, Y. Feldman, M. Homyonfer, H. Cohen, J. Sloan, J. L. Hutchison, R. Tenne, Wear **225-229**, 975 (1999).

[22] L. Rapoport, N. Fleischer, R. Tenne, Advanced Materials **15**, 651(2003).

[23] L. Rapoport, Y. Bilik, Y. Feldman, M. Homyonfer, S. R. Cohen, R. Tenne, Nature **387**(19), 791 (1997).

[24] H. B. Yang, S. K. Liu, J. X. Li, M. H. Li, G. Peng, G. T. Zou, Nanotechnology **17**, 1512 (2006).

[25] L. L. Zhang, J. P. Tu, H. M. Wu, Y. Z. Yang, Materials Science and Engineering A **454-455**, 487 (2007).

[26] J. F. Wu, W. S. Zhai, G. F. Jie, Tribology International **43**, 1650 (2010).
[27] N. Wu, N. N. Hu, G. B. Zhou, J. H. Wu, Journal of Experimental Nanoscience **13**(1), 27 (2018).
[28] X. H. Zhang, H. X. Xu, J. T. Wang, X. Ye, W. N. Lei, M. Q. Xue, H. Tang, C. S. Li, Nanoscale Research Letters **11**, 442 (2016).
[29] M. Nath, A. Govindaraj, C. N. R. Rao, Advanced Materials **13**(4), 283 (2001).
[30] X. H. Zhang, W. N. Lei, X. Ye, C. Wang, B. C. Lin, H. Tang, C. S. Li, Materials Letters **159**, 399 (2015).
[31] E. S. Vasilyeva, O. V. Tolochko, B. K. Kim, D. W. Lee, D. S. Kim, Microelectronics Journal **40**, 687 (2009).
[32] S. X. Cao, C. Zhao, L. L. Peng, Materials Letters **65**, 3164 (2011).
[33] H. A. Therese, J. X. Li, U. Kolbb, W. Tremel, Solid State Sciences **7**, 67 (2005).
[34] S. X. Cao, T. M. Liu, W. Zeng, S. Hussain, X. H. Peng, Micro & Nano Letters **10**(3), 183 (2015).
[35] W. Li, D. H. Chen, F. Xia, J. Z. Y. Tan, J. C. Song, W. G. Songe, R. A. Caruso, Chemical Communications **52**, 4481 (2016).
[36] D. Q. Zhang, T. T. Liu, J. Y. Cheng, S. Liang, J. X. Chai, X. Y. Yang, H. Wang, G. P. Zheng, M. S. Cao, Ceramics International **45**, 12443 (2019).
[37] X. H. Zhang, M. Q. Xue, X. H. Yang, G. S. Luo, F. Yang, Micro & Nano Lett. **10**, 7 (2015).
[38] G. Zhao, Q. Zhao, W. Li, X. Wang, W. Liu, Lubr. Sci. **26**, 1 (2014).
[39] L. Rapoport, M. Lvovsky, I. Lapsker, W. Leshchinsky, Y. Volovik, Y. Feldman, R. Tenne, Wear **249**, 150 (2001).